applied sciences

MDPI

Article

The Dependence of Ultrasonic Velocity in Ultra-Low Expansion Glass on Temperature

Wenqing Wei [1,2], Yongfeng Zhang [1,3], Zongzheng Du [1], Minwei Song [1], Yuanyuan Zhang [1,*] and Hong Liu [1,2,*]

[1] Institute of Optics and Electronics, Chinese Academy of Sciences, Chengdu 610209, China; weiwenqing15@mails.ucas.ac.cn (W.W.); zhangyongfeng15@mails.ucas.edu.cn (Y.Z.); 13739450124@163.com (Z.D.); 18780175291@139.com (M.S.)
[2] University of Chinese Academy of Sciences, Beijing 100049, China
[3] Key Laboratory of Adaptive Optics, Chinese Academy of Sciences, Chengdu 610209, China
* Correspondence: zhangyy@ioe.ac.cn (Y.Z.); liuh972@sina.com (H.L.)

Abstract: The coefficient of thermal expansion (CTE) is an important property of ultra-low expansion (ULE) glass, and the ultrasonic velocity method has shown excellent performance for the nondestructive measurement of CTE in large ULE glass. In this method, the accurate acquisition of the ultrasonic velocity in ULE glass is necessary. Herein, we present a correlation method to determine the ultrasonic TOF in ULE glass and to further obtain the ultrasonic longitudinal wave velocity (c_L) indirectly. The performance of this method was verified by simulations. Considering the dependence of c_L on temperature (T), we carried out the derivation of the analytical model between c_L and T. Based on reasonable constant assumptions in the physical sense, a c_L–T exponential model was produced, and some experimental results support this model. Additional experiments were carried out to validate the accuracy of the c_L–T exponential model. The studies we conducted indicate that the c_L–T exponential model can reliably predict the ultrasonic velocity in ULE glass at different temperatures, providing a means for the nondestructive CTE measurement of large ULE glass at a specified temperature.

Keywords: ultra-low expansion glass; ultrasonic velocity; correlation method; temperature coefficient; exponential model

Citation: Wei, W.; Zhang, Y.; Du, Z.; Song, M.; Zhang, Y.; Liu, H. The Dependence of Ultrasonic Velocity in Ultra-Low Expansion Glass on Temperature. *Appl. Sci.* **2022**, *12*, 577. https://doi.org/10.3390/app12020577

Academic Editors: Phong B. Dao, Lei Qiu, Liang Yu and Zahra Sharif Khodaei

Received: 6 December 2021
Accepted: 31 December 2021
Published: 7 January 2022

1. Introduction

Ultra-low expansion (ULE) glass is a SiO_2–TiO_2 glass formed by flame hydrolysis and vapor deposition (nominal composition: 93 wt% SiO_2 and 7 wt% TiO_2) that has found applications in large telescope mirror blanks because of its near-zero coefficient of thermal expansion (CTE) over the 5~35 °C temperature range [1,2]. However, the uniformity of glass material has a significant impact on the CTE homogeneity of the final ULE glass products, which results in figure distortion and in the degradation of the optics. It is therefore necessary to know the CTE characteristics of ULE glass to better understand—and thus better control—the fabrication process for manufacturing the highest quality ULE boules.

Commonly used methods for measuring the CTE of ULE glass include the pushing-rod dilatometer [3], interferometric [4,5], and photoelastic analysis [6–8] methods. All involve destructive measurements, and the procedures are time-consuming and expensive, so they are not suitable for the detection of the CTE uniformity of large ULE glass. The ultrasonic velocity in ULE glass is proportional to its CTE, a fact that can be utilized to nondestructively assess the absolute and relative CTE of large ULE glass, and its feasibility has been demonstrated by researchers [9,10]. In the process of using ultrasonic velocity to nondestructively detedmine CTE, there are two key points to focus on. One is how to guarantee high accuracy in the ultrasonic velocity measurements, and the second is the

correspondence between CTE and ultrasonic velocity at certain given temperatures, mainly because both ultrasonic velocity and CTE are temperature-dependent characteristics.

For the first point, the ultrasonic velocity can be measured by various effective methods, including the threshold method [11,12], the zero-crossing method [13], the peak method [14,15], and the correlation approach [16,17]. The first three methods are based on using the local signal characteristics to measure physical quantities, and the measurement findings are strongly reliant on local signal characteristics and are easily influenced by human factors (such as subjectively selected thresholds) or noise. By contrast, the correlation method considers global signals, which contribute to its excellent noise robustness, and it is free of subjective effects. In this study, we use the correlation method to accurately measure the ultrasonic velocity in ULE glass.

We now turn to the dependence of ultrasonic velocity on temperature. The use of ultrasonic velocity measurements to characterize the CTE of ULE glass was first discovered by researchers at Corning. In their research, some troublesome operations and correction models were used to achieve nondestructive CTE testing [10]. On the one hand, the internal physical mechanism is not very clear. On the other hand, the various cumbersome practical steps (including ensuring the constant temperature of the sample to reach thermal equilibrium, removal of the water bath, quick-drying, and ultrasonic velocity measurement [9]) can introduce uncertainty regarding the sample temperature, which, in turn, affects the accuracy of the CTE measurement results. In later research, the tested sample is not forcefully separated from the constant temperature water bath during ultrasonic CTE measurement [18], which reduces the CTE measurement error, but this also increases the time cost of the entire measurement. Herein, we have analytically modeled the influencing mechanisms, which will help to simplify the practical procedures.

The paper is organized as follows. The principle and method of ultrasonic velocity measurement are mathematically stated in the following section. Section 3 summarizes the derivation of the dependence of ultrasonic velocity on temperature. Section 4 describes the composition of an ultrasonic velocity measurement system and the preparation of the tested samples in detail. In Section 5, the uncertainty and stability of the ultrasonic velocity measurement are discussed, the experimental establishment of the ultrasonic velocity–temperature exponential model is presented, and a comparison of the predicted ultrasonic velocity with the actual measured ultrasonic velocity is listed. Finally, the conclusions are presented in Section 6.

2. Principle and Method of Ultrasonic Velocity Measurement

2.1. Principle of the Ultrasonic Velocity Measurement

Many instruments are now employed to measure ultrasonic velocity, most of which use the pulse reflection method [19–21]. This method usually involves time-domain analysis based on the ultrasonic time of flight (TOF). In this analysis, the ultrasonic velocity is obtained by the ratio of the material thickness to the ultrasonic TOF [13,22]. On this basis, we built a fully integrated high-precision system to measure the ultrasonic velocity in ULE glass using the immersion pulse reflection method.

Figure 1 depicts the schematic diagram of the immersion pulse reflection method. The time of S_F relative to the time base "0" point is called t_1. The time interval between B_1 and S_F is recorded as Δt_1, and the time interval between B_2 and B_1 is recorded as Δt_2, which have the following relationship:

$$\begin{aligned} t_1 &= 2H/c_L^{\text{water}}, \\ \Delta t_1 = \Delta t_2 &= 2d/c_L^{\text{sample}}. \end{aligned} \tag{1}$$

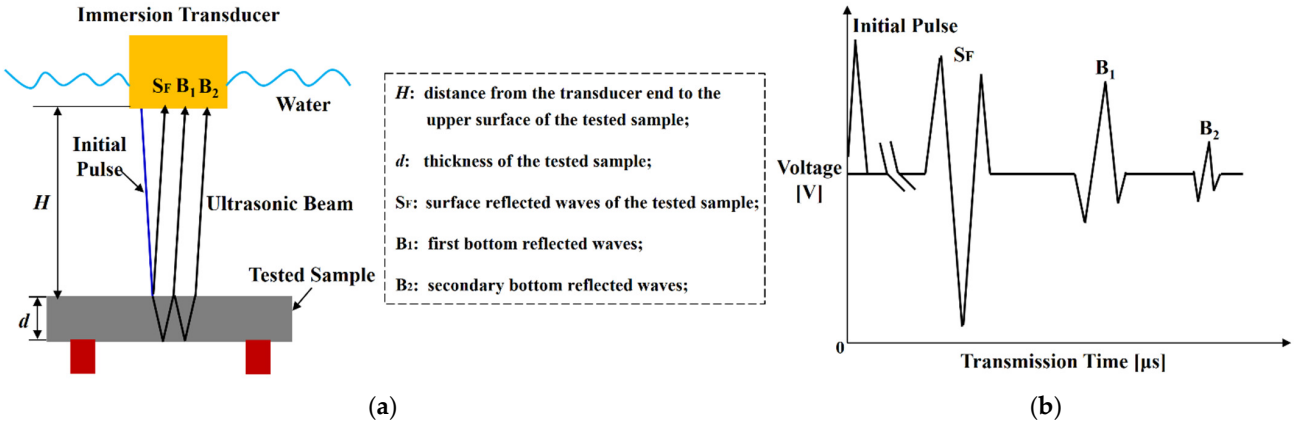

Figure 1. Schematic diagram of the immersion pulse reflection method: (**a**) the transmission process of ultrasonic waves; (**b**) the transmission time of ultrasonic waves.

The ultrasonic longitudinal wave velocity (c_L) of a sample can be calculated from Equation (1):

$$c_L^{\text{sample}} = 2d/\Delta t_1 = 2d/\Delta t_2. \quad (2)$$

Using Equation (2), we can determine the c_L of the tested sample by first determining Δt_1 or Δt_2 of the ultrasonic waveform and the known thickness d.

2.2. Correlation Method for Measuring the TOF

2.2.1. The Correlation Calculation Principle

As the B_1 and B_2 signals of the ULE samples were readily available and were highly similar, the correlation method was used to determine the time interval between B_1 and B_2 as the ultrasonic TOF in the samples. In detail, the ultrasonic signal that was sampled and saved in the PC is designated as $x(t)$. By separating the B_1 and B_2 signals and noting them as $x_1(t)$ and $x_2(t)$, respectively, the correlation coefficient (R) can be represented as

$$R = \frac{\int_{-\infty}^{+\infty} x_1(t)x_2(t)\mathrm{d}t}{\sqrt{\left[\int_{-\infty}^{+\infty} x_1^2(t)\mathrm{d}t \int_{-\infty}^{+\infty} x_2^2(t)\mathrm{d}t\right]}} (|R| \le 1). \quad (3)$$

The ultrasonic signals that were collected by the data acquisition card and the PC, on the other hand, were two discrete signal arrays. As a result, for the discrete signals, the normalized R can be given as

$$R = \frac{\sum x_1(i)x_2(i) - \sum x_1(i)\sum x_2(i)/n}{\sqrt{\left(\left[\sum x_1^2(i) - (\sum x_1(i))^2/n\right]\left[\sum x_2^2(i) - (\sum x_2(i))^2/n\right]\right)}}, i = 1, 2, \ldots, n. \quad (4)$$

where n is the computed length of the signal array, and i is the location inside the signal array.

In the time domain of signal $x(t)$, there is a time interval between the signals $x_1(t)$ and $x_2(t)$. The time interval between $x_1(t)$ and $x_2(t)$ is the round trip time of the ultrasonic wave propagated in the thickness direction, i.e., the TOF. Equation (4) is used to generate the correlation array, with the position having the largest correlation coefficient corresponding to the temporal position of m. The corresponding TOF (Δt) is equal to m/f_S if the sampling frequency is noted as f_S. Finally, the following equation can be used to calculate the ultrasonic velocity:

$$c_L = \frac{2d \cdot f_S}{m}. \quad (5)$$

2.2.2. Simulation of the Correlation Method

First, the reliability of the proposed algorithm needed to be validated by simulations in which the simulated ultrasonic signal is a declining sinusoidal function.

$$x(t) = \beta \cdot \exp(-\alpha_s t) \cdot \sin(2\pi f_c t) \quad (6)$$

where α_s is the declining coefficient of the sinusoidal function set as 9×10^6 Np/m; f_c is the center frequency of the ultrasonic transducer set as 5 MHz; β is the amplitude of the signal; and the amplitudes of the initial and echo signals are set to 1 and 0.3 V, respectively.

The sampling frequency of the signal was set as 2.5 GHz, and the TOF between the initial and echo signals was set as 17.36 µs. To come closer to the actual measurement signal, Gaussian noise with +15 dB SNR (Signal-to-Noise Ratio) was added to the ideal declining sinusoidal signal. The simulated signal waveform and the correlation distribution calculation results are shown in Figure 2a,b, respectively.

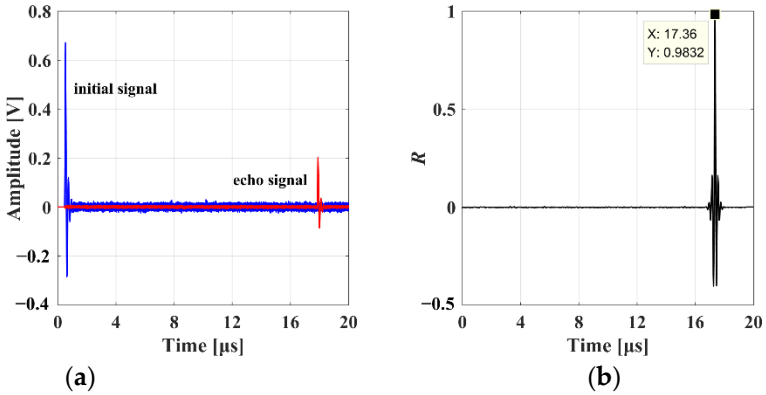

Figure 2. The correlation calculation result of a simulated signal: (**a**) the waveform of the simulated signal; (**b**) the correlation coefficient distribution.

Where the X value is the time corresponding to the largest correlation coefficient, and the Y value is the largest correlation coefficient.

In Figure 2, the calculated correlation coefficient has a clear peak on the time axis, with a TOF of 17.36 µs corresponding to the peak. The calculated results were in good agreement with the theoretical settings, so the algorithm is suitable for ultrasonic signal processing in ultrasonic velocity measurements.

3. Theoretical Model between Ultrasonic Velocity and Temperature

Ultrasound is defined as an elastic wave of high frequency that propagates in a medium. Therefore, when an elastic wave propagates in an isotropic medium without being affected by volume stress, the ultrasonic longitudinal wave velocity, denoted as c_L, can be found from the following equation:

$$c_L = \sqrt{\frac{E(1-v)}{\rho(1+v)(1-2v)}}, \quad (7)$$

where ρ is density, v is Poisson's ratio, and E is Young's modulus.

Equation (7) indicates that the c_L in the material is mainly related to Young's modulus, density, and Poisson's ratio. For ULE glass, within the upper limit of 11.5 wt%, slight changes in the TiO_2 content will not change the density or Poisson's ratio but will cause changes to Young's modulus [23]. Therefore, the difference in c_L is mainly determined by the difference in Young's modulus. Then, the effect of temperature on the ultrasonic velocity essentially reflects its effect on Young's modulus. The microscopic analysis of Young's modulus shows that the reaction of a solid to all forces comes from the potential

energy of the interaction between atoms. The interaction potential $U(r)$ of a pair of two atoms separated by r can be expressed as:

$$U(r) = -\frac{A}{r^n} + \frac{B}{r^m}, \tag{8}$$

where A, B, n, and m are all positive constants. The first term represents the energy of attraction, and the second term represents the energy of repulsion.

Assuming that the solid is stretched along the crystal axis when the tensile force changes df, the interatomic distance r changes to dr. At this time, the cross-sectional area r^2 of a unit cell is regarded as inconvenient. Then, Young's elastic modulus can be expressed as:

$$E = \frac{\sigma}{\varepsilon} = \frac{\frac{\mathrm{d}f}{r^2}}{\frac{\mathrm{d}r}{r}} = \frac{\mathrm{d}f}{r\mathrm{d}r}, \tag{9}$$

where σ and ε represent the stress and strain, respectively.

Since the binding force f of the tensioned solid is only related to the first term of Equation (8), its magnitude is:

$$f(r) = -\frac{\mathrm{d}U(r)}{\mathrm{d}r} = -\frac{nA}{r^{n+1}}. \tag{10}$$

Equation (10) is then substituted into Equation (9) by deriving the derivative for r to obtain

$$E = \frac{n(n+1)A}{r^{n+3}}. \tag{11}$$

Assume $K = (n + 1)\ A$ and $Q = n + 3$. Equation (11) can be changed to:

$$E = \frac{nK}{r^Q}. \tag{12}$$

Equation (12) takes the derivative of T and divides both sides by Er^Q at the same time, shifting the term to obtain:

$$\frac{\mathrm{d}E}{E\mathrm{d}T} = Q\frac{\mathrm{d}r}{r\mathrm{d}T}. \tag{13}$$

It is assumed that the distance between atoms still obeys the following rules when a solid is heated and expanded:

$$r = r_0(1 + \alpha T), \tag{14}$$

where r_0 is the atomic distance when the absolute temperature $T_0 = 0$; α is the linear expansion coefficient of the solid, and its differential definition is:

$$\begin{cases} \alpha = \frac{1}{r}\frac{dr}{dT}, \eta = \frac{1}{E}\frac{dE}{dT}. \end{cases} \tag{15}$$

The η in Equation (15) is the temperature coefficient of the elastic modulus. Relevant studies have demonstrated that the elastic modulus of ULE glass increases with the increase in temperature, and the increment dE of E has a positive value [23]. When both sides of Equation (13) are multiplied by dT, Equation (14) is then substituted in and integrated, and we obtain:

$$\int_{E_0}^{E} \frac{\mathrm{d}E}{E} = Q\int_{T_0}^{T} \frac{\mathrm{d}(1+\alpha T)}{(1+\alpha T)}. \tag{16}$$

From Equation (16) and considering $T_0 = 0$, we obtain:

$$E = E_0\left(\frac{1+\alpha T}{1+\alpha T_0}\right)^Q \approx E_0(1 + Q\alpha T). \tag{17}$$

From Equations (13) and (15), we see that:

$$Q{=}\eta/\alpha. \tag{18}$$

Therefore, Equation (17) is changed to:

$$E = E_0(1 + \eta T). \tag{19}$$

Equation (19) shows that the elastic modulus of ULE glass increases as the temperature increases, where η is the temperature coefficient of the elastic modulus. Therefore, it can be inferred that the c_L in ULE glass also increases as T increases. A review of the data reveals that when considering the effects of thermal expansion, there is a specific equation relating the c_L and T, which is as follows [24]:

$$c_L^T = c_L^{T_0}[1 + \alpha_L(T - T_0)], \tag{20}$$

where α_L is the temperature coefficient of the ultrasonic longitudinal wave velocity, a positive value of about 10^{-4} orders of magnitude, and c_L^T, $c_L^{T_0}$ indicate the ultrasonic longitudinal wave velocity of the material at temperatures T and T_0, respectively.

Although there are certain differences in α_L at different temperature points, we can use the c_L–T data in a small temperature range to fit and solve the average α_L in this temperature range. The method of a differential equation is introduced here to obtain the mathematical relationship between c_L and T in a small temperature range. Writing Equation (20) in a differential form, we obtain

$$\alpha_L = \frac{dc_L}{c_L dT},\ T_1 < T < T_2. \tag{21}$$

Solving this equation yields

$$c_L = c' \cdot e^{\alpha_L T}. \tag{22}$$

Equation (22) shows that the relationship between c_L and T is theoretically exponential within a certain temperature range.

4. Tested Material and Experimental Setup

4.1. Materials and Sample Preparation

The selected ULE glass was Corning Code 7972 glass. Considering the boundary effect of ultrasonic wave propagation, the experimental samples were prepared in a cylindrical shape with a cross-sectional area that was larger than that of the ultrasonic transducer. To avoid the adverse effects of the scattering attenuation of ultrasound at the interface of the sample, the two end faces of the tested sample should be flat and parallel to each other. As shown in Figure 3, six cylindrical glass samples were cut with an equal thickness (50–0.1 mm) along the radial position of the ULE 7972 boule (No. 82714) using an abrasive water jet; then, these samples were finely ground and polished to achieve a flatness of 0.5λ and parallelism of 20 μm. The six samples were numbered 1#~6# from the inside to the outside of the boule according to the increasing CTE. The details of the ULE samples are summarized in Table 1.

4.2. Ultrasonic Measurement System

The schematic diagram of the c_L. measurement experimental system is illustrated in Figure 4. A 75 MHz ultrasonic pulser/receiver (Olympus, Waltham, MA, USA, model 5073PR) was used, which was connected to a 400 MHz data acquisition card (Spectrum Instrumentation GmbH, Grosshansdorf, Germany, model M4i.2220-x8) that transmits the ultrasonic signals to a computer to be processed. All signals were captured with 2,500,000 points at a sampling rate of 2.5 GHz. After the acquisition, the data were properly processed to determine the involved ultrasonic velocities. The temperature of the tested

sample was controlled by a thermostatic water tank (Hangzhou Qiwei, Hangzhou, China, model DHC-05-B) with a temperature control precision of ±0.05 °C.

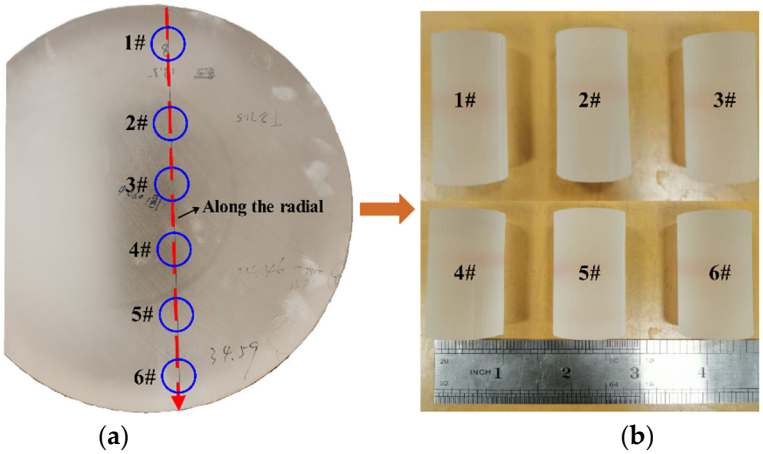

Figure 3. The prepared ULE glass samples: (**a**) source of samples; (**b**) photograph of samples.

Table 1. The important parameters of the ULE samples.

No.	Thickness (mm)	CTE (5~35 °C) (ppb/°C)
1#	49.936	−1
2#	49.932	0
3#	49.937	1
4#	49.940	2
5#	49.941	2
6#	49.927	3

Note: No.—sample number; thickness—measured thickness of the ULE samples; CTE (5~35 °C)—average CTE over the temperature range 5~35 °C; ppb/°C—unit of CTE (1 ppb/°C = 1 × 10^{-9}/°C).

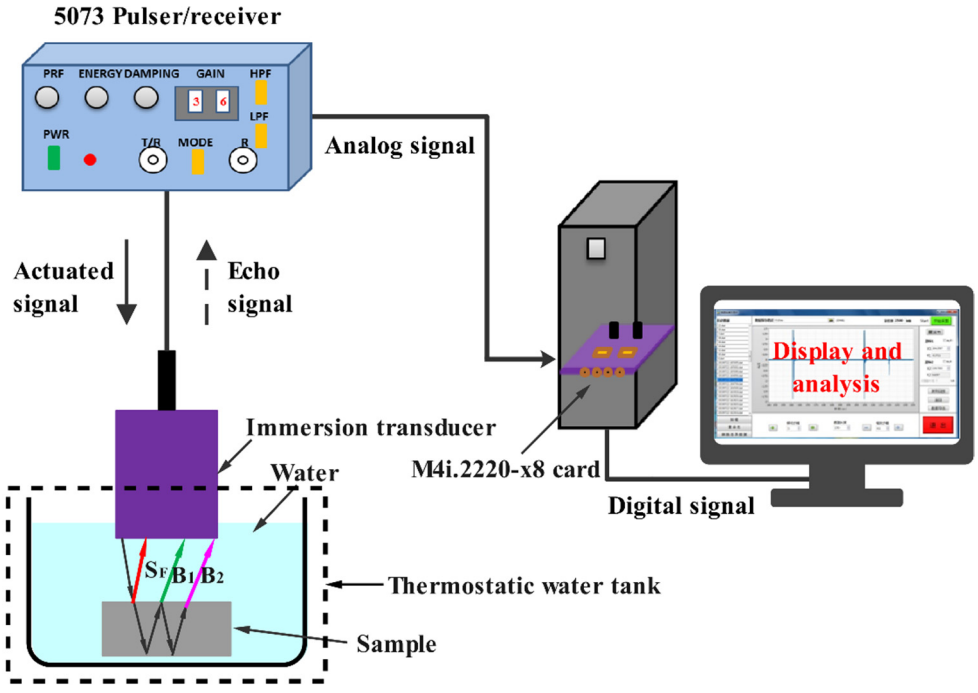

Figure 4. Schematic diagram of the experimental system for measuring ultrasonic velocity.

The self-generating and self-receiving transducer model was utilized to transmit and receive the ultrasonic waves. Considering the diameter and thickness of the tested sample, wideband focusing 19.05 mm diameter longitudinal wave immersion transducers (Olympus, Waltham MA, USA) with 3.5 and 5 MHz nominal center frequencies were employed in this investigation. Figure 5 illustrates the ultrasonic velocity measurement results for the samples 1#~6# at 20 °C using two different ultrasonic frequencies: 3.5 and 5 MHz. Each sample was subjected to five replicate measurements by each transducer. The ultrasonic frequency had little effect on the ultrasonic velocity of the sample, as the c_L in the sample only depends on its inherent physical parameters, including its bulk modulus and density [25]. In addition, the repeatability of the c_L measurement was essentially the same for both frequency transducers, both within 0.1 m/s. This suggests that any frequency could be used to characterize the CTE of ULE glass in engineering applications when using ultrasonic velocity measurement methods.

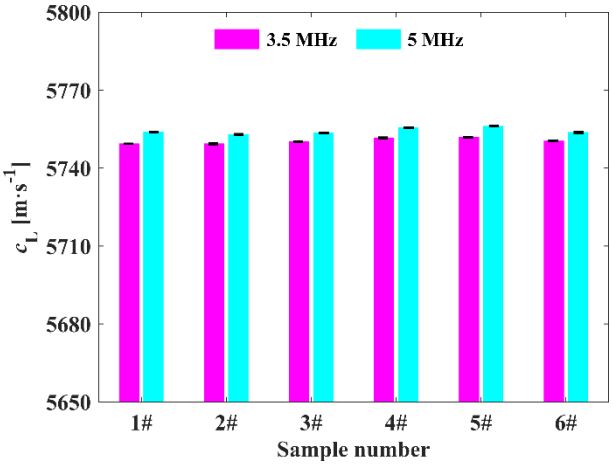

Figure 5. c_L measurement results of the ULE samples 1#~6# at frequencies of 3.5 and 5 MHz.

5. Results and Discussion

5.1. c_L Measurement at a Single Temperature

5.1.1. Uncertainty Analysis

In this work, an ultrasonic transducer with a 5 MHz center frequency was employed to measure the ultrasonic velocities in all of the prepared ULE samples. Figure 6 gives an example of the received ultrasonic signals, which formed a series of ultrasonic longitudinal waves with a sampling rate of 2.5 GHz. High-frequency noise was found to be present in the actual ultrasonic signals. However, since the correlation of the noisy signal was very small, the effect of such noise was removed via the correlation calculation. The results of the TOF calculations obtained using this method are depicted in Figure 6. Again, there is a peak in the correlation coefficient distribution plot corresponding to a TOF of Δt = 17.3383 µs.

The uncertainty in measuring ultrasonic velocity was also investigated, and the expression is shown in Equation (23).

$$u_{c_L} = \sqrt{\left(\frac{2}{\Delta t}u_d\right)^2 + \left(\frac{2d}{(\Delta t)^2}u_{\Delta t}\right)^2} \tag{23}$$

where u_{c_L}, u_d, and $u_{\Delta t}$ are the uncertainties regarding the c_L, d, and TOF in the ULE glass, respectively.

As illustrated in the first item of Equation (23), the uncertainty related to the d was $u_{c_L}(d) = (2/\Delta t)\Delta u_d$. A typical value of Δt is 17.3562 µs. When measuring the d of the ULE sample, u_d was evaluated by the measurement precision of a micrometer (0.001 mm), thus $u_{c_L}(d) = 0.12$ m/s. After substituting the measured values into the second item of Equation (23), the uncertainty introduced by the TOF (Δt) was obtained: $u_{c_L}(\Delta t) = 0.332 \times 10^9 u_{\Delta t}$.

Since $u_{\Delta t}$ was evaluated by the sampling period of the data acquisition card (0.4 ns), the typical $u_{c_L}(\Delta t)$ was 0.13 m/s. Therefore, when measuring the ULE glass using the proposed experimental setup, the calculated total uncertainty was $u_{c_L} = 0.2$ m/s, ensuring that the ultrasonic velocity measurements at a single temperature had high reliability.

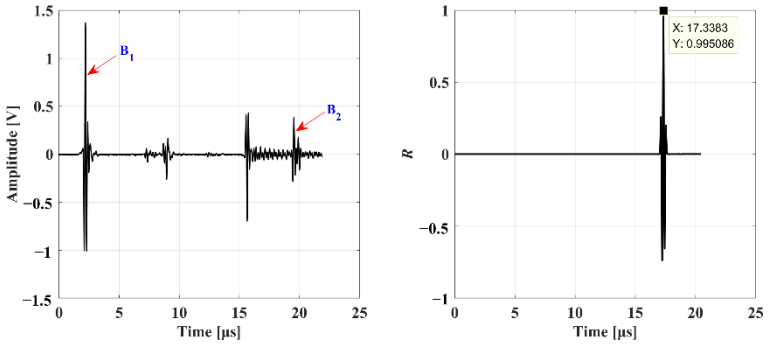

Figure 6. The correlation calculation result of an actual received ultrasonic signal: (**a**) the ultrasonic echo signal; (**b**) the correlation coefficient distribution.

5.1.2. Stability of c_L Measurement

To determine whether the proposed measurement system could provide reliable c_L measurements over long periods of time, the stability of the measured c_L value also needs to be considered when the tested samples reach thermal equilibrium. Long-term measurement of the ultrasonic velocity in samples 1#~6# with a high CTE was taken at the same temperature (20 °C), and the c_L data were recorded at 1 h intervals, for a total of seven measurements in one day. Figure 7 depicts the variation in c_L with the measurement time.

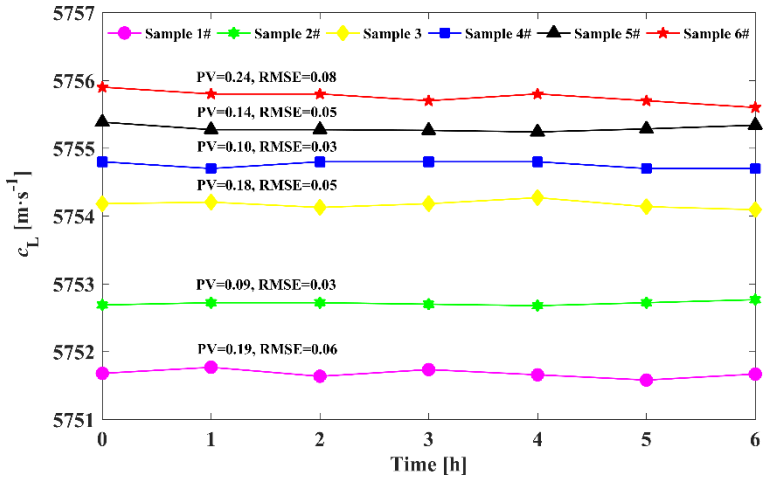

Figure 7. The change in c_L with time for samples 1#~6#.

The c_L measured in the same sample was almost constant at the different times while maintaining a constant temperature, and the RMSE (Root Mean Squared Error) of the c_L changes were all within 0.10 m/s, which indicate that the measurement system that was built in this paper has stable performance. This also provides a strong guarantee for the c_L measurement of a large batch of ULE glass samples.

5.2. Measurement and Analysis of c_L–T Data

5.2.1. Acquisition of c_L–T Data

The tested sample and an ultrasonic transducer fixed above the sample were placed into a thermostatic water tank, and the temperature in the tank was steadily increased

in the range of 10~30 °C. Here, the temperature range of 10~30 °C was chosen for two reasons: (1) this corresponds to the real temperature range that ULE glass is likely to experience when undergoing ultrasonic measurements, i.e., the range of room temperature throughout the year, and (2) it corresponds to the temperature range of the ultrasonic transducer in use. We were utilizing a standard immersion transducer, whose normal operating temperature range is 10~60 °C, beyond which the piezoelectric action of the transducer would be weakened, making high-amplitude data acquisition difficult. The ultrasonic echo signals were manually sampled and stored by the PC at a temperature interval of 1 °C, which was chosen to account for the maximum number of temperature points to be sampled and the required modeling time. The temperature was held constant within ±0.05 °C, as measured using a digital thermometer probe in the bath.

To ensure that the glass sample was in thermal equilibrium during the TOF measurement, the sample was immersed in a controlled water bath for at least 94 min, which was calculated according to the time t (hours) to reach equilibrium for a given glass thickness d (cm), which could be expressed as $t = d^2/16$ in [26]. To reduce measurement errors, the echo signals were acquired three times at each temperature point. By using the described correlation algorithm method, the ultrasonic TOF was obtained, and the average values were used to calculate the c_L of the tested ULE samples. Nevertheless, the experiment did not consider the change in the d and ρ of the tested samples.

The obtained ultrasonic velocities of samples 1#~6# are presented in Figure 8 in terms of temperature. The ultrasonic velocities are observed to increase as the temperature increases. Changes in c_L are correlated with temperature changes, regardless of the absolute value of the CTE. Comparing Figure 8a–f, we can also observe that the ultrasonic velocity differs at the same temperature and that the c_L increases with the CTE of ULE glass.

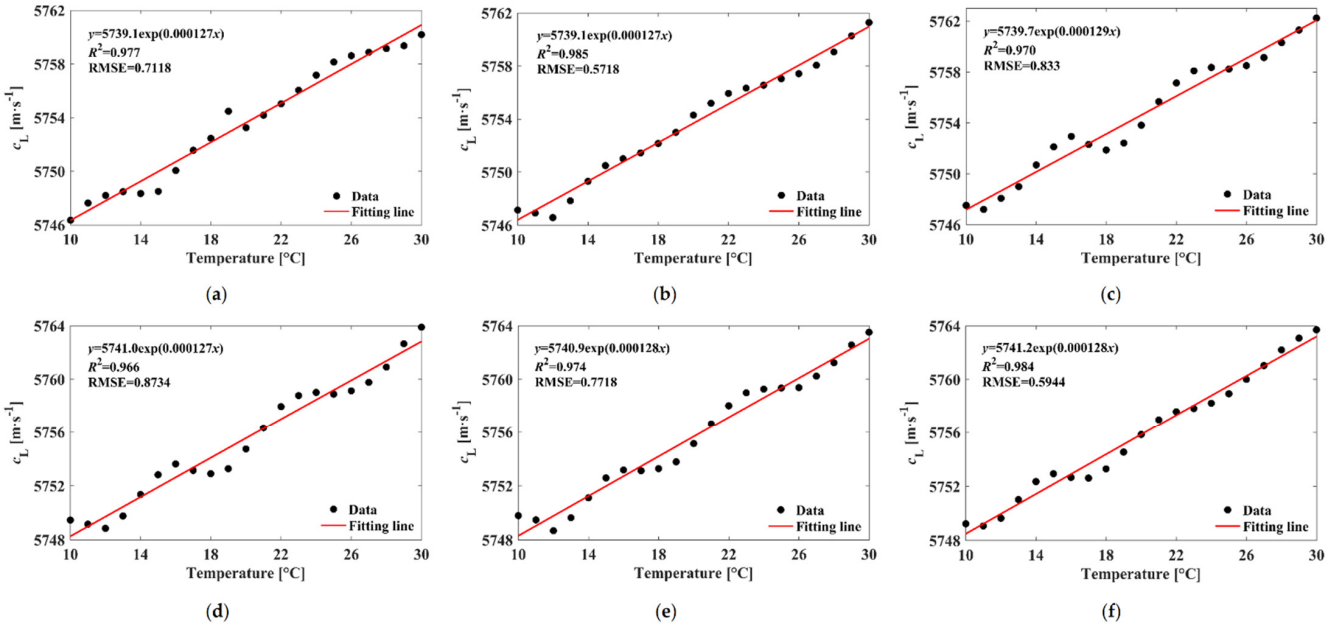

Figure 8. Changes in c_L(m·s^{-1}) with temperature for all measured samples: (**a**) sample 1#; (**b**) sample 2#; (**c**) sample 3#; (**d**) sample 4#; (**e**) sample 5#; (**f**) sample 6#.

5.2.2. Analysis of the Change in the c_L with T

The data from Figure 8 were used to directly plot the changes in c_L as a function of T according to the exponential fitting in Equation (22). Table 2 displays the results of all six samples, with excellent exponential fits given for each case and with α_L mostly ranging from 0.000127 to 0.000129, which shows that for ULE materials with very small CTE differences, their α_L is almost constant. This means that the temperature effect pattern on ultrasonic velocity was essentially the same in ULE glasses with different CTE values.

Therefore, the average value of these α_L coefficients could be taken as the temperature correction coefficient of ultrasonic velocity in ULE glass. Of course, because of the small difference in the CTE, the c' in Equation (22) showed relatively large fluctuations. In the physical sense, the c' indicates that c_L correpsonds to 0 °C. It was found that as the CTE of the ULE sample increased, c' increased correspondingly, which is consistent with the mechanism of the linear positive correlation between c_L and the CTE.

Table 2. Data from the six samples shown in Figure 8 were taken to exponentially fit the relationship between c_L and T.

No.	$\alpha_L/\times 10^{-6}$	R^2	RMSE
1#	127	0.977	0.7118
2#	127	0.985	0.5718
3#	129	0.970	0.8330
4#	127	0.966	0.8734
5#	128	0.974	0.7718
6#	128	0.984	0.5944

Note: No.—sample number; α_L—temperature coefficient of ultrasonic longitudinal wave velocity; R^2—R-square (a measure of goodness of fit).

To represent the more pronounced difference in the ultrasonic velocity with increasing temperature for the ULE samples with different CTE values, a new coefficient is defined as follows:

$$\beta_L = \frac{\Delta c_L}{c_L \Delta T}. \quad (24)$$

Here, we take the c_L corresponding to 10 °C of the samples as the basis c_L, and calculate the β_L via Equation (24) with temperature increments of 5 °C, i.e., at 15 °C, 20 °C, 25 °C, and 30 °C. The β_L for samples 1#, 2#, and 3# is shown in Figure 9. We noted that for the different temperature ranges, the speed of the ultrasonic velocity changes with the temperature was inconsistent. This is possibly because the elastic modulus also has a temperature coefficient β_E, which varies in different temperature ranges. The PV value of β_L for the three samples was 0.000098, 0.000056, and 0.000101. Considering that the difference was minor, we conclude that the multi-data point fitting method that was used to obtain α_L in a given temperature range in this paper is a more feasible equivalent to an average function and has wider temperature applicability.

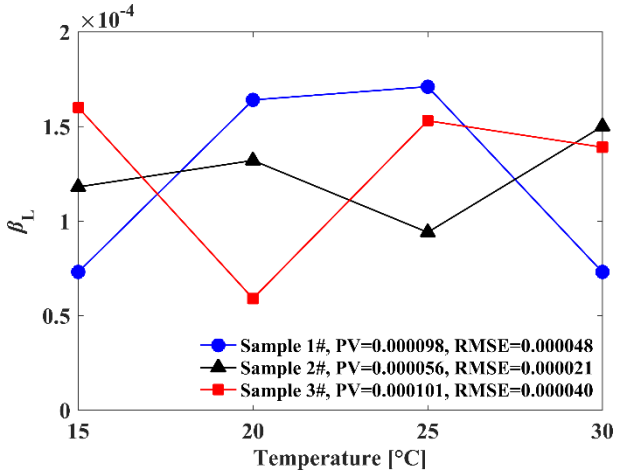

Figure 9. The relationship between β_L and temperature for ULE samples with different CTEs.

Samples 4# and 5#, which had the same CTE, were also analyzed for differences in the c_L as the temperature increased, and the results are shown in Figure 10. We found that the two samples had similar patterns of variation in β_L. This implies that the changing trends in the ultrasonic velocity with temperature was, to some extent, consistent with the

changing trend of the CTE with temperature; however, this assumes that the thickness of the ULE glass sample did not change over a wide temperature range.

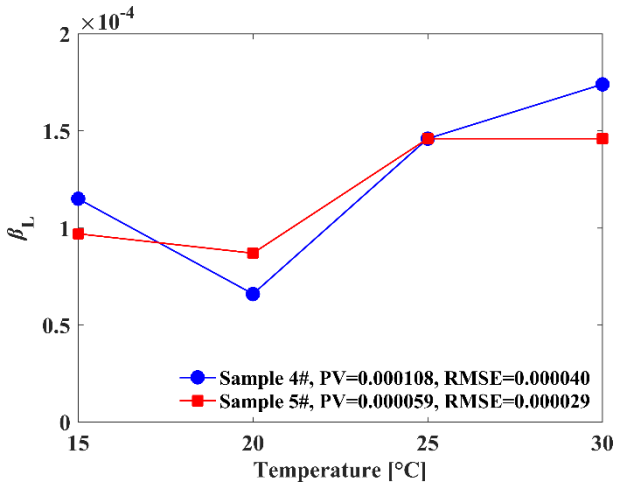

Figure 10. The relationship between β_L and temperature for ULE samples with the same CTE.

The correlation between c_L and T in ULE glass over a wide range of CTE values from −1 ppb/°C to +3 ppb/°C was investigated and discussed. We will next validate the accuracy of the c_L–T exponential model for ULE samples with different CTE values through a series of experiments.

5.3. Accuracy Validation of c_L–T Model

The accuracy of the c_L–T model was decisive for its application in engineering. Samples 1#, 3#, and 5# were randomly selected, and their ultrasonic velocities were measured at ten random temperature points in the range of 10~30 °C. The measured values were compared with the model predictions in this paper, and the results are shown in Table 3.

Table 3. Experimental data from the model validation and their error analysis.

No.	Temperature (°C)	c_m(m/s)	c_p(m/s)	$c_m - c_p$(m/s)	|δ| %
1#	10.2	5745.5	5746.3	−0.8	0.014
	12.7	5748.1	5748.2	−0.1	0.002
	14.3	5749.6	5749.3	0.3	0.005
	15.2	5749.4	5750.0	−0.6	0.010
	17.6	5750.3	5751.7	−1.4	0.024
	21.8	5754.4	5754.8	−0.4	0.007
	23.5	5754.9	5756.1	−1.2	0.021
	25.6	5457.1	5757.6	−0.5	0.009
	26.0	5757.5	5757.9	−0.4	0.007
	27.9	5759.4	5759.3	0.1	0.002
				σ_c = 0.75	
3#	10.8	5747.5	5746.8	0.7	0.012
	12.4	5747.9	5748.0	−0.1	0.002
	15.2	5751.7	5750.1	1.6	0.028
	16.5	5751.5	5751.0	0.5	0.009
	16.9	5751.4	5751.3	0.1	0.002
	18.4	5751.5	5752.4	−0.9	0.016
	23.3	5757.3	5756.1	1.2	0.021
	24.3	5757.2	5756.8	0.4	0.007
	25.6	5757.5	5757.8	−0.3	0.005
	29.0	5761.1	5760.3	0.8	0.014
				σ_c = 0.85	

Table 3. Cont.

No.	Temperature (°C)	c_m(m/s)	c_p(m/s)	$c_m - c_p$(m/s)	$\|\delta\|$ %
5#	10.6	5750.4	5749.7	0.7	0.012
	11.3	5750.2	5750.2	0.0	0.000
	13.5	5752.1	5751.8	0.3	0.005
	14.1	5753.1	5752.3	0.8	0.014
	15.1	5754.4	5753.0	1.4	0.024
	17.5	5754.2	5754.8	−0.6	0.010
	20.3	5756.8	5756.8	0.0	0.000
	25.2	5760.3	5760.5	−0.2	0.003
	25.9	5760.4	5761.0	−0.6	0.010
	29.9	5764.8	5763.9	0.9	0.016
				σ_c = 0.73	

Note: c_m is the actual measured ultrasonic velocity, c_p is the ultrasonic velocity predicted by the fitting model, and δ denotes the relative error. The deviation σ_c is a measure of the inaccuracy.

Considering that the measurement locations of the three samples in the model validation procedure may vary, it was reasonable to use a recalculation of $c^{'}$ based on the standard ultrasonic velocity at 20 °C to determine the c_L–T exponential model, which may differ slightly from the $c^{'}$ obtained by modeling the above c_L–T data. The c_L values in the tested glasses at an average room temperature of 20 °C were substituted into the derived exponential model based on the average temperature coefficient from the above fitting analysis to determine a c_L–T exponential model for each tested glass. As seen in Table 3, the standard deviation of the predicted values for three samples were all within 0.90 m/s, and the relative errors between measured and model-predicted values were mostly within 0.020%, which suggests that the models fitted in this work exhibit high precision.

Of course, it should be noted that increasing the sample thickness may further reduce the errors in c_L measurement, but it also imposes more stringent requirements on the frequency of the transducer and time required for the sample to reach thermal equilibrium.

6. Conclusions

In this investigation, the aim was to theoretically analyze and validate the dependence of the ultrasonic velocity in ULE glass on temperature. Based on the simulation and experimental investigations, we can draw the following conclusions:

1. The proposed pulse reflection immersion method provides reliable and stable measurements of the ultrasonic echo signal of ULE glass, and the calculation of the signal based on the correlation method can be used to conveniently and accurately extract the ultrasonic TOF of the tested sample and then obtain the ultrasonic velocity.
2. The application of the proposed method for six ULE samples with different CTE values indicates that ultrasonic velocity increases as the experimental temperature is increased. Furthermore, the c_L–T exponential model was theoretically analyzed and experimentally fitted. The predicted c_L using the exponential model at ten random temperature points shows good agreement with the actual measured ultrasonic velocities at the same temperature.

These findings indicate the promising potential of the c_L–T exponential model to determine the ultrasonic velocity at a specified temperature for ultrasonic nondestructive CTE measurement in large ULE glass, which will be critical for reliably evaluating the CTE homogeneity of large ULE glass at a specified temperature.

There are some comments that can be made about the general applicability of our method. In this paper, the derivation and verification of the c_L–T relationship are only for isotropic ULE glass, but the method for deriving exponential model can also be applied to anisotropic materials, such as anisotropic crystals, and for obtaining the longitudinal wave velocity, transverse wave velocity, and then the Poisson's ratio. The only distinction is α_L. As for the experimental verification method for the exponential model, the correlation

method, it is also applicable for the measurement of the TOF, regardless of whether the material is isotropic.

Author Contributions: Conceptualization, W.W., Y.Z. (Yuanyuan Zhang) and H.L.; methodology, Y.Z. (Yongfeng Zhang) and H.L.; software, W.W. and Y.Z. (Yongfeng Zhang); validation, W.W. and H.L.; investigation, W.W. and M.S.; resources, Y.Z. (Yuanyuan Zhang), M.S. and H.L.; data curation, W.W.; writing—original draft preparation, W.W.; writing—review and editing, Y.Z. (Yongfeng Zhang), Z.D. and H.L.; visualization, W.W.; project administration, Y.Z. (Yuanyuan Zhang). All authors have read and agreed to the published version of the manuscript.

Funding: This research received no external funding.

Institutional Review Board Statement: Not applicable.

Informed Consent Statement: Not applicable.

Data Availability Statement: Not applicable.

Conflicts of Interest: The authors declare no conflict of interest.

References

1. VanBrocklin, R.R.; Edwards, M.J.; Wells, B. Review of Corning's capabilities for ULE mirror blank manufacturing for an extremely large telescope. In Proceedings of the SPIE—The International Society for Optical Engineering, Orlando, FL, USA, 6 July 2006; Volume 6273, p. 627301.
2. Kendrick, S.E.; Stahl, H.P. Large aperture space telescope mirror fabrication trades. In Proceedings of the SPIE—The International Society for Optical Engineering, Marseille, France, 12 July 2008; Volume 7010, p. 70102G.
3. Plummer, W.A.; Hagy, H.E. Precision thermal expansion measurements on low expansion optical materials. *Appl. Opt.* **1968**, *7*, 825–831. [CrossRef]
4. Imai, H.; Okaji, M.; Kishii, T.; Sagara, H.; Aikawa, H.; Kato, R. Measurement of thermal expansivity of low-expansion glasses by interferometric methods: Results of an interlaboratory comparison. *Int. J. Thermophys.* **1990**, *11*, 937–947. [CrossRef]
5. Kato, R.; Azumi, T.; Maesono, A. Measurement of thermal expansion of low-expansion glasses by a laser interferometric thermal expansion meter. *High Temp.-High Press.* **1991**, *23*, 615–620.
6. Hagy, H.E.; Smith, A.F. Sandwich seal in the development and control of sealing glasses. *J. Can. Ceram. Soc.* **1969**, *38*, 63–68.
7. Hagy, H.E.; Best, M.E. Comparison of two high-precision nondestructive measurement methods for evaluating thermal expansion differences in the 8.3-m ultralow-expansion Subaru primary mirror blank. *Appl. Opt.* **1996**, *35*, 1126–1128. [CrossRef]
8. Gulati, S.T.; Hagy, H.E. Theory of the narrow sandwich seal. *J. Am. Ceram. Soc.* **2006**, *61*, 260–263. [CrossRef]
9. Hagy, H.E. High precision photoelastic and ultrasonic techniques for determining absolute and differential thermal expansion of titania–silica glasses. *Appl. Opt.* **1973**, *12*, 1440–1446. [CrossRef] [PubMed]
10. Hagy, H.E.; Shirkey, W. Determining absolute thermal expansion of titania–silica glasses: A refined ultrasonic method. *Appl. Opt.* **1975**, *14*, 2099–2103. [CrossRef] [PubMed]
11. Barshan, B. Fast processing techniques for accurate ultrasonic range measurements. *Meas. Sci. Technol.* **2000**, *11*, 45–50. [CrossRef]
12. Xia, N.; Zhao, P.; Zhang, J.; Xie, J.; Fu, J. Investigation of ultrasound velocity measurements of polymeric parts with different surface roughness. *Polym. Test.* **2020**, *81*, 106231. [CrossRef]
13. Zhao, P.; Peng, Y.; Yang, W. Crystallization measurements via ultrasonic velocity: Study of poly (lactic acid) parts. *J. Polym. Sci. Part B Polym. Phys.* **2015**, *53*, 700–708. [CrossRef]
14. Jenot, F.; Ouaftouh, M.; Duquennoy, M.; Ourak, M. Corrosion thickness gauging in plates using Lamb wave group velocity measurements. *Meas. Sci. Technol.* **2001**, *12*, 1287–1293. [CrossRef]
15. Kim, Y.H.; Song, S.J.; Lee, J.K. Technique for measurements of elastic wave velocities and thickness of solid plate from access on only one side. *Jpn. J. Appl. Phys.* **2005**, *44*, 5240–5243. [CrossRef]
16. Hu, E.; Wang, W. The elastic constants measurement of metal alloy by using ultrasonic nondestructive method at different temperature. *Math. Probl. Eng.* **2016**, *2016*, 6762076. [CrossRef]
17. Zhao, P.; Xia, N.; Zhang, J. Measurement of molecular orientation using longitudinal ultrasound and its first application in in-situ characterization. *Polymer* **2020**, *187*, 122092. [CrossRef]
18. Edwards, M.J.; Bullock, E.H.; Morton, D.E. Improved precision of absolute thermal expansion measurements for ULE glass. In Proceedings of the SPIE—The International Society for Optical Engineering, Denver, CO, USA, 11 November 1996; Volume 2857, pp. 58–63.
19. Leydier, A.; Mathieu, J.; Despaux, G. The two coupling fluids method for ultrasonic velocity measurement. Application to biological tissues. *Meas. Sci. Technol.* **2009**, *20*, 095801. [CrossRef]
20. Souri, D. Ultrasonic velocities, elastic modulus and hardness of ternary Sb-V_2O_5-TeO_2 glasses. *J. Non-Cryst. Solids* **2017**, *470*, 112–121. [CrossRef]

21. Minh, H.N.; Du, J.; Raum, K. Estimation of thickness and speed of sound in cortical bone using multifocus pulse-echo ultrasound. *IEEE Trans. Ultrason. Ferroelectr. Freq. Control* **2019**, *67*, 568–579. [CrossRef] [PubMed]
22. Daugschies, M.; Rohde, K.; Glüer, C.C.; Barkmann, R. The preliminary evaluation of a 1 MHz ultrasound probe for measuring the elastic anisotropy of human cortical bone. *Ultrasonics* **2014**, *54*, 4–10. [CrossRef] [PubMed]
23. Gulati, S.T. Mechanical properties of SiO_2 vs. SiO_2-TiO_2 bulk glasses and fibers. *MRS Online Proc. Libr.* **1991**, *244*, 67–84. [CrossRef]
24. Jiang, Z. Effect of temperature on ultrasonic velocity and stress measurement (in Chinese). *Nondestruct. Test.* **1999**, *21*, 245–248.
25. Perepechko, I.; Leib, G. *Acoustic Methods of Investigating Polymers*; Mir Publishers: Moscow, Russia, 1975.
26. Lillie, H.R.; Ritland, H.N. Fine annealing of optical glass. *J. Am. Ceram. Soc.* **1954**, *37*, 466–473. [CrossRef]